

FabHydro: Printing Interactive Hydraulic Devices with an Affordable SLA 3D Printer

Zeyu Yan

Department of Computer Science, University of Maryland,
College Park
College Park, MD, USA
zeyuy@umd.edu

Huaishu Peng

Department of Computer Science, University of Maryland,
College Park
College Park, MD, USA
huaishu@umd.edu

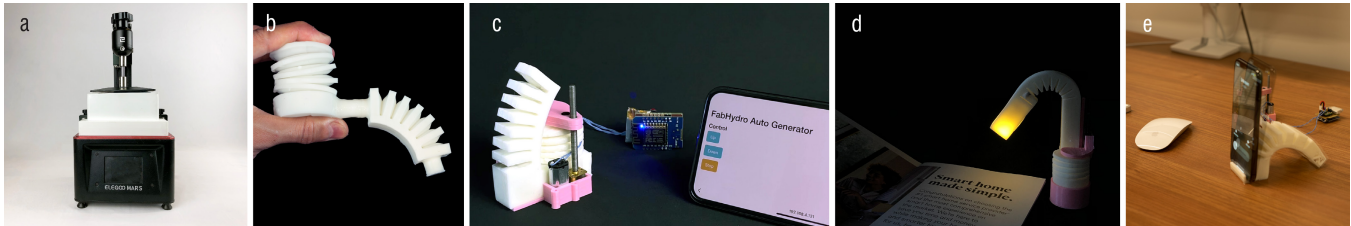


Figure 1: FabHydro overview: a) an off-the-shelf SLA printer with a modified tank and printing plate; b) a complete hydraulic device with a bellows generator and a bending actuator connected with a short piece of tubing; c) a bending actuator is activated by an automatic generator; d) a printed lamp lights up with the change of its posture; e) a phone stand acts as an ambient display when the phone rings.

ABSTRACT

We introduce *FabHydro*, a set of rapid and low-cost methods to prototype interactive hydraulic devices based on an off-the-shelf 3D printer and flexible photosensitive resin. We first present printer settings and custom support structures to warrant the successful print of flexible and deformable objects. We then demonstrate two printing methods to seal the transmission fluid inside these deformable structures: the *Submerged Printing* process that seals the liquid resin without manual assembly, and the *Printing with Plugs* method that allows the use of different transmission fluids without modification to the printer. Following the printing methods, we report a design space with a range of 3D printable primitives, including the hydraulic generator, transmitter, and actuator. To demonstrate the feasibility of our approaches and the breadth of new designs that they enable, we showcase a set of examples from a printed robotic gripper that can be operated at a distance to a mobile phone stand that serves as a status reminder by repositioning the user's phone. We conclude with a discussion of our approach's limitations and possible future improvements.

CCS CONCEPTS

• **Human-centered computing** → **Interactive systems and tools**; **Interaction devices**.

Permission to make digital or hard copies of all or part of this work for personal or classroom use is granted without fee provided that copies are not made or distributed for profit or commercial advantage and that copies bear this notice and the full citation on the first page. Copyrights for components of this work owned by others than ACM must be honored. Abstracting with credit is permitted. To copy otherwise, or republish, to post on servers or to redistribute to lists, requires prior specific permission and/or a fee. Request permissions from permissions@acm.org.

UIST '21, October 10–14, 2021, Virtual Event, USA

© 2021 Association for Computing Machinery.

ACM ISBN 978-1-4503-8635-7/21/10...\$15.00

<https://doi.org/10.1145/3472749.3474751>

KEYWORDS

Fabrication, 3D Printing, Interaction, Design

ACM Reference Format:

Zeyu Yan and Huaishu Peng. 2021. FabHydro: Printing Interactive Hydraulic Devices with an Affordable SLA 3D Printer. In *The 34th Annual ACM Symposium on User Interface Software and Technology (UIST '21)*, October 10–14, 2021, Virtual Event, USA. ACM, New York, NY, USA, 14 pages. <https://doi.org/10.1145/3472749.3474751>

1 INTRODUCTION

One of the long-term visions for additive manufacturing is to print devices with functionalities and interactivities [51]. For example, recent research has shown different approaches to print interactive components, including 3D speakers that generate sound with diaphragm coating [20], light bulbs that are printed with custom light channels using transparent material [3], and touch sensors with conductive thermoplastic [39]. They allow 3D printed objects to have sound, light, and sensing capabilities, but these printed objects cannot move.

To offer mechanical motion, recent research looks for ways of incorporating mechanical actuators into the printed object — some use pre-manufactured actuators [15]; others aim to print actuators directly. For example, Peng et al. [32] design a custom 3D printer that can embed magnetic wires into the printing process to build reluctant motors. MacCurdy et al. [25] propose to seal droplets inside a printed cavity to make hydraulic walking robots. These approaches show the potential to print one-off objects with mechanical motion, but the fabrication process remains challenging. They either require custom 3D printers with complex hardware designs such as a five-degree-of-freedom printing platform, or require high-end industrial 3D printers with multi-material printability. These machines often cost over 200,000 US dollars and are not accessible by many.

In this paper, we propose *FabHydro*, a set of fabrication methods to democratize the printing of hydraulic-driven mechanical devices with consumer-grade 3D printers that cost less than 200 US dollars. Our core idea centers on low-cost stereolithography (SLA) printers, which can produce both stiff and flexible structures from a selected photosensitive resin in one printing process. We first present the overall strategies and the printing material selections that warrant the successful print of flexible and deformable structures. These structures require special printing supports to overcome the local adhesive force formed at each new layer that may cause failed printing.

We then detail two optional printing processes that seal the hydraulic liquid inside. With the first process, which we called *Submerged Printing*, the entire hydraulic device, including the mechanical and the fluid inside, can be printed all at once. This is suitable for printing hydraulic prototypes for fast design iteration, as the printed device requires no manual assembly and is ready to test out-of-the-printer. However, this process requires modifications to the off-the-shelf printer and thus might be overwhelming for novices. The operation should also be taken with precaution, as the fluid inside the printed structure is uncured resin. The second process, which we called *Printing with Plugs*, allows the user to fill water or other liquids inside the printed chamber and seal them with printed plugs as a post-process. The benefit of this method is that it requires no hardware modification to the printer. However, printed objects require manual assembly.

Following the printing methods, We provide a systematic design space and guidelines to use hydraulic components as building blocks. These building blocks include the printed hydraulic generator, transmitter, and actuator. We present geometric parameters and constraints of them based on a series of controlled mechanical experiment. The design guidelines can help users go through a successful design of a complete hydraulic device. To highlight the potential of *FabHydro*, we showcase a series of 3D printed examples: see Figure 20 - Figure 23 and our supplementary Video Figure.

In summary, our paper contributes: (i) a set of new methods to print flexible and deformable structures with two liquid sealing techniques; (ii) a systematic design space for a complete printed hydraulic device; and (iii) multiple functional applications showcasing how the building blocks in the design space can be featured in hydraulic systems and various use cases of interactive hydraulic devices.

2 RELATED WORK

Our work builds upon the notion of 3D printing of functional artifacts. Specifically, we will discuss three research thrusts, including printing with embedded foreign objects, printing with custom fabrication machines, and printing functional objects with smart materials and structures.

2.1 Printing with Embedded Foreign Objects

As noted by Ashbrook et al. [2], one approach to fabricate functional artifacts is to embed off-the-shelf components into a 3D printed housing. Savage et al. [37] and Hook et al. [15] propose to embed a web camera and wireless IMUs respectively to detect input

motions; Steel-Sense [46] utilizes microcontrollers to detect conductivity changes in customized machined mechanical hardware. One common challenge for these approaches is to design the 3D printed housing so that the final artifact has an appealing look while holding foreign components reliably. To ease the design process, Savage et al. [38] introduce a two-step design pipeline, where end-users use clay to craft the 3D housing first and then 3D print the scanned version of it for the final product. To simplify the assembly process, Gao et al. [12] propose to enclose all electronics into a standardized laser-cut box and then print 3D housing around it. Zhu et al. [52] further illustrate the idea to embed custom breadboards into 3D printed objects to allow greater flexibility during the prototyping phases. The aforementioned work uses off-the-shelf sensors and electronics to imbue interactivity to 3D printed artifacts. While using foreign objects can offer a wide variety of functionalities, the design process still requires careful planning to ensure components fitting; the integration process also requires manual engagement, which can be time-consuming, and inevitably introduce human error.

2.2 Printing with Custom Fabrication Machines

Another approach to print functional objects is to imbue sensing and actuation using custom machines other than off-the-shelf 3D printers. For example, various modifications have been made to FDM printers to embed new materials. These include machines that use electrospinning to print soft textiles [36], use a modular dispenser to print smart material [50], and use multi-nozzle printing head, that in combined with multi-material, to print sophisticated functional devices such as walking robots [41]. Other printer mechanisms have also been explored for functional 3D printing. For example, Katakura et al. [23] include additional rigid jigs aside from a printer head to create functional objects without post-print assembly. Peng et al. [33] introduce a layered 3D printer design to print touch sensors and antennas with conductive fabric sheets. Peng et al. [32] propose printer hardware that composes a five-degree-of-freedom platform and a duo wire feeder. In combination, the printer can build electromagnetic devices during the 3D printing process.

In our work, we will introduce two methods to seal hydraulic liquids, *Submerged Printing* and *Printing with Plugs*. Among these, the *Submerged Printing* process requires hardware modifications to an off-the-shelf 3D printer, in a similar vein to the device modifications mentioned above. However, our hardware modification is low-cost, as we only suggest a new vat design and a printing plate extension, which can be manufactured by experienced DIYers.

2.3 Printing Functional Objects with Smart Materials and Structures

Recent work also explores how the structures of a printed object can introduce sophisticated mechanical functionalities. For example, various strand-structures (DefeXtiles [11], Kim et al. [44], Ou et al. [29], and Laput et al. [24]) have been introduced to print flexible objects; custom spring constraints and bi-stable structures (Ondulé [14] and Pop-up Print [28]) have been explored to print objects that can store and release energy. Ion et al. propose a series of works

[16–19] that use meta-material structures to achieve mechanically-sound printed artifacts.

Research has also examined functional printing using unique material properties. For example, [1, 13, 48, 49] show how to print shape-changing objects by taking advantage of the shape memory effect of PLA. Capricate [39], Printput [4], and BodyPrinter [5] show how to print custom capacitive sensors by using the conductive property of metallic filament or ink. Willis et al. [51] propose to print tubing structures using transparent material for interactive lighting and sensing.

Beyond the field of HCI, researchers in robotics have proposed various methods ([6, 25, 31, 40, 47]) to print or cast pneumatic or hydraulic driven robotic structures. Among which, Printable hydraulics [25] might be the one that is closest to our work. In this work, researchers fabricate hydraulic structures utilizing the liquid phase of the material in 3D inkjet printing [43]. The printed structures require no post assembly and can be used for rapid prototyping of mechanical functional objects. In the similar vein, our goal is also to print functional hydraulic devices, but with several differences. First, we utilize a low-cost printing method – SLA, which has been widely used in the HCI community and is cost-effective. In fact, the SLA printer we used cost less than 200 US dollars, 1000 times cheaper than the industrial inkjet printer [42] used in [25]. Second, we introduce a series of technical contributions that are unique to SLA printing. For example, we overcome the natural printing instability caused by the flexible material. We also introduce two printing methods to embed liquid inside a printed object. Finally, we present a systematic design space for printable hydraulic devices, aiming to support designers to quickly make and customize hydraulic-driven mechanical prototypes.

3 PRINTING HYDRAULIC DEVICE

A hydraulic device is a drive system that uses fluid as the medium to transfer energy from the source of the actuation to an actuator [10]. Compared to other transmission mechanisms such as hard mechanical transmission and pneumatic transmission [30], a hydraulic system transfers energy with low impact, rapid speed, and high density.

A standard hydraulic device consists of three parts: a generator (e.g., a hydraulic pump) that is driven by an external force such as an electric motor, a transmission system with valves, filters, and piping, and an actuator to operate the machinery. This paper focuses on hydraulic systems, including the generator, transmitter, and actuator, that can be 3D printed with single material using an affordable SLA 3D printer.

Figure 2a illustrates one example of our 3D printed hydraulic device. It includes a compressible bellows that acts as the generator, a bending actuator, and a piece of tube that connects both ends and

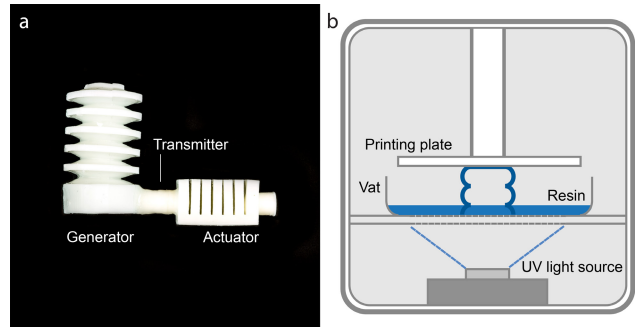


Figure 2: a) An overview of one *FabHydro* device, including a generator, a short piece of tubing, and a bending actuator; b) the conventional SLA printer with single material and an upside-down printing process.

with locked-in resin as the transmission fluid. The entire structure is solid but flexible and is printed one-off. When an external force compresses the generator, the incompressible liquid inside the generator will be driven towards the linear actuator via the tube; the chambers of the actuator will take the fluid and expand against one another to generate the bending motion.

The system is printed with an Elegoo Mars LCD-SLA 3D Printer [8] with the F39/F69 flexible photosensitive resin from RESIONE [35]. As illustrated in Figure 2b, an SLA printer has three main components, the ultraviolet (UV) light source that is installed to its bottom, a vat with a transparent foil (FEP) that is above the light source and contains liquid resin, and a building plate where a 3D model is printed upside-down from its surface.

To print hydraulic structures with an SLA printer, we face several challenges. Since the hydraulic structure needs to be compressible, the common choice of the resin material will not work for the flexible generator and actuator structure. The automatically generated supporting structures will also result in failed printing. Finally, the default printer hardware cannot print sealed structures with locked-in liquid. In the following sections, we will detail our methods that ensure the successful fabrication of a hydraulic device, such as the set shown above.

3.1 Printing Material

We experimented with three different types of resin: the standard photosensitive resin [9], the Siraya Tech Tenacious resin [45] (one of the most accessible flexible resins on the market), and the F39/F69 resin from RESIONE [35]. The goal is to find the resin that can be used to print deformable structures, i.e., structures that are both compressible and stretchable.

Table 1: Material behaviors and properties

	Shore	Elongation Break Ratio	Compression	Elongation	Rebound
<i>StandardResin</i>	84D	14.2%	N/A	N/A	N/A
<i>TenaciousResin</i>	65D	75%	good	poor	poor
<i>F39/F69Resin</i>	75A	255.1%	good	good	good

To understand the flexibility of the selected materials, we printed a set of hollow bellows with 1 mm wall thickness with all three materials (Figure 3a). The one printed with the standard resin cracked under loads before any noticeable deformation (Figure 3c), suggesting that it will not fulfill our goal despite being widely available. The Tenacious resin is performing better in compression than the standard resin, as the model could be compressed with obvious deformation. However, the rebound speed is slow due to the stiffness, and the elongation of the model is limited by the elongation at the break ratio of the material (Figure 3b). Thus, this impact-resistant resin is not ideal as hydraulic systems require faster rebound and better stretchability. With the same testing model, the sample printed with F39/F69 resin can be compressed to half the length and extended to 1.5 times the length without breaking (Figure 3d and e), making it an ideal candidate for printing hydraulic devices. See Table 1 for the summary of the material properties and behaviors.

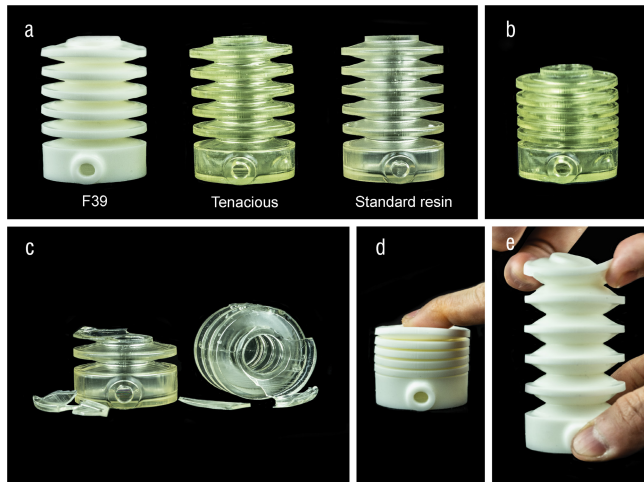


Figure 3: Materials: a) testing samples printed with the standard resin (right), the Siraya Tenacious resin (middle), and the F39 resin (left); b) the Tenacious sample comes with slow rebound; c) the standard resin model fails the compression test; d) the F39 model can be easily compressed; e) the F39 model is easily extended.

Besides flexible structures, a working hydraulic system also needs certain spots to remain strong and rigid to serve as structural supports. As the Poisson effect suggests, the thicker the material gets, the stronger it is to resist deformation. We thus further explored how the deformation is affected by the structure thickness of models printed with the F39/F69 resin.

Figure 4a shows nine testing samples with a rectangular cross-section (20 mm × 30 mm) and a thickness ranges from 1 mm to 5.5 mm, with a 0.5 mm increment. We fixed one end of the samples and engaged a load of 0.49 N at the other end. Figure 4b shows the bending angle versus the thickness in the given dimension of the printed samples. We conclude that a printed wall with a thickness of 3 mm can serve the purpose of a stiff structure, while a wall with less than 2 mm can create a hinge with great flexibility. All models

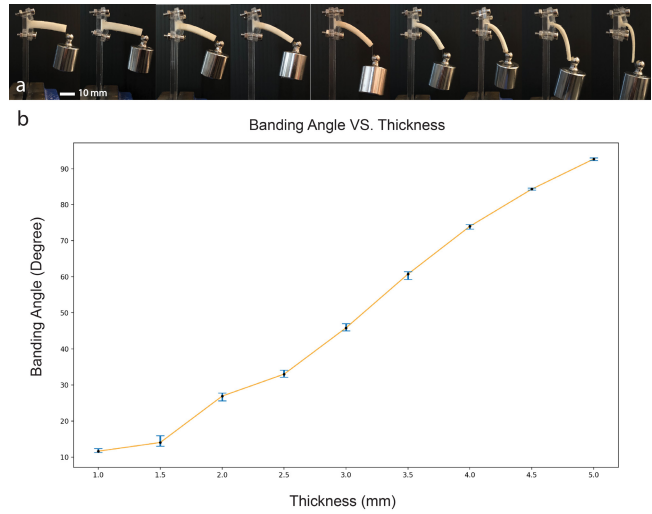


Figure 4: Bending angle test: a) models were bent under loads; b) the thickness vs the bending angle of the testing samples.

in the rest of the paper are printed with the F39/F69 flexible resin unless otherwise noted.¹

3.2 Printing Deformable Structures

The flexible F39/F69 resin allows us to print 3D structures with both flexible and stiff structures. However, in practice, a custom setting and supporting structures are needed to ensure a successful print.

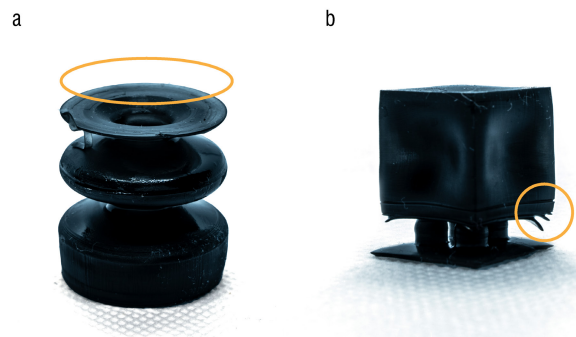


Figure 5: Two typical failed cases: 1) a bellows is only printed half way through because of the elongation of the overall structure; 2) a cube testing case fails because of the loose bonding between layers.

¹F39 is the flexible resin in white color and F69 is the same resin in black. We use both to print examples in this paper.

3.2.1 Understanding Failed Printing. Figure 5a and b show two failed examples using the flexible resin. Notice that both models would be printed successfully without support using the standard resin, as all new layers can stick to their previous one even with an overhang structure, as long as there is no isolated island.

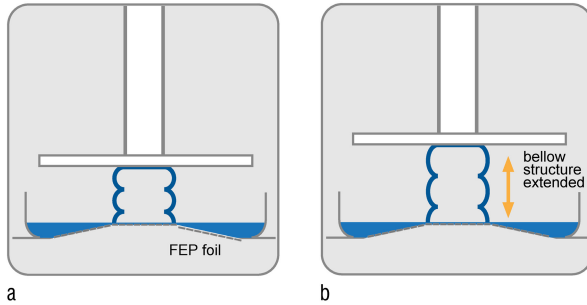


Figure 6: a) Printed layer peels from the FEP foil; b) an elastic structure absorbs the peeling force.

To understand why these prints failed, we revisit the details of the SLA printing process. In SLA printing, each new layer is cured between the transparent FEP foil window and the last layer printed. Because the new layer tends to stick to the FEP foil, a lifting motion of the printing plate is required to detach the new layer from the FEP. During the lifting, the FEP is slightly bulged up, creating peeling edges at the newly printed layer, which separates the printed object and the FEP foil (Figure 6a). This process works well when both the cured layer and the already printed structure are rigid. However, with the deformable hydraulic structure (such as the bellows structure in Figure 6b) and the flexible resin, two types of errors may be introduced during the process.

Elongated Part: The hydraulic device’s deformable structure will not detach from the FEP foil with normal lifting force; instead, it tends to elongate. Since most of the energy is absorbed by the elongation, the part would not be successfully peeled off from the FEP foil (Figure 6b).

Large Overhangs: Large areas overhanging surfaces can also cause failed printing. Instead of maintaining the shape like what the standard resin part does, new layers printed with flexible resin are not well constrained during printing. The lifting process moves printed parts up and down periodically. The soft ‘skirt’ surfaces that are not well-overlapped with the previous layer will thus float following the up and down motion irregularly, creating a potentially unstable substrate for the next layer to be cured upon. When cumulated, these unstable surfaces may introduce potential breaks during a later layer’s detaching process.

To conclude, to successfully fabricate hydraulic structures, we need to prevent structure-wised deformation during the printing process and enhance the bonding between layers.

3.2.2 Supports for Flexible and Elongated Structure. To ensure the printed structure with minimum elongation, we add additional support panels across the potentially extended area enabled by

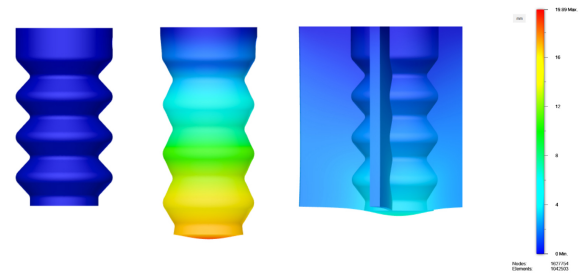


Figure 7: A simulation of the bellows structure with the standard resin (left), the flexible resin (middle), and the flexible resin with panelized supporting structures (right). The panel supports limit the deformation along the longitudinal axis, make the bellows printable.

Finite Element Analysis (FEA) simulation (Figure 7). Boundary conditions are applied to simulate the lifting process: the top surface is constrained to simulate the printing plate; the bottom surface is applied with a uniformly distributed load to simulate the adhesive force between the part and the FEP foil. We add the panel support for all models that will extend a large amount of deformation (threshold being 20 mm) in the printing process. Note that we deliberately make the support panel solid to mitigate any potential deformation along the longitudinal axis. The solid panel supports can be easily trimmed off using a pair of cutters.

3.2.3 Support for Better Edge Bonding. To overcome the second type of error, we modify the settings for the tree support structures generated with the printer’s default slicing software CHITUBOX. We increase the support density from 30% to 80%. For each of the tree structure, we change the following parameters: contact diameter from 0.8 mm to 1.6 mm, contact depth from 0.4 mm to 0.8 mm, connection dimension from 0.4 mm (upper diameter) - 1.2 mm (lower diameter) to 1.6 mm - 2.8 mm respectively, connection length from 2 mm to 3 mm, and cylinder pillar diameter from 1.2 mm to 3 mm. If necessary, we add support structures at certain corners and boundaries additional to the auto-generated supports.

3.2.4 Exposure Time and Lifting Speed. To further increase the bonding and reduce the chance of error at each of the printed layers, we adjust the default UV light exposure time and the lifting speed after the exposure per layer. Based on our experiments, we increase the exposure time for each layer from 8 s to 30 s and use 50 s exposure time for the first several layers; we decrease the building plate lifting speed from the default setting of 90 mm/min to 55 mm/min. The increase of the exposure time and the decrease of the lifting time will slow down the overall printing speed, but can ensure a better bonding between the first layer to the building plate, and among the rest of the printed layers. Note that the reported setting is only a suggestion to the Elagoo Mars 3D printer, but can be used as a reference starting point for other desktop SLA printers.

3.3 Sealing Hydraulic Fluid

Aside from printing deformable structures, we also need to seal hydraulic fluid inside the printed structures; it can happen while printing or afterward. We now present each of the processes.

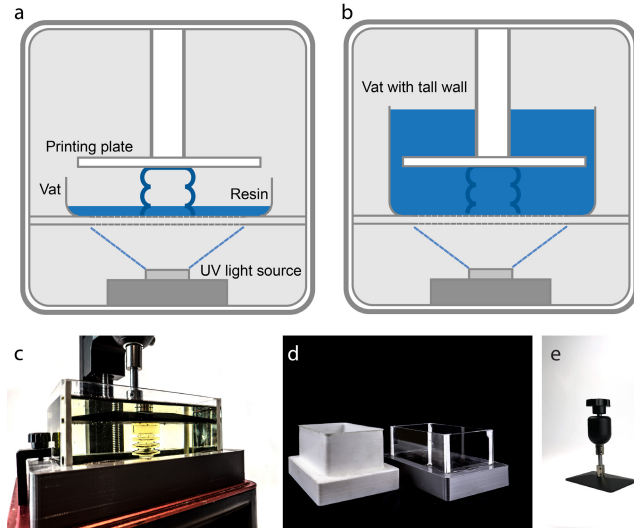


Figure 8: a) The conventional SLA 3D printer structure; b) the *Submerged Printing* process; c) the modified printer assembly filled with standard transparent resin for a clear presentation; and d) the modified vat made with PLA and acrylics; e) the extended printing plate.

3.3.1 Submerged Printing. With the *Submerged Printing* technique, we aim to print a complete liquid-sealed hydraulic device with minimum post process. This requires lightweight modifications to the current 3D printer hardware. With the conventional SLA printer setup, the bottom of the model remains open until the end of the entire printing process (Figure 8a). Thus, the liquid resin will flow out from the printed structure’s bottom open-end. Our solution is to make the printing process as a whole happens below the liquid level (Figure 8b and c). The model is still ‘grow’ upside-down from the printing plate but will not be pulled out of the liquid until the print is finished.

Specifically, we propose a low-cost modification with a new vat design with an 88 mm wall height that allows 80 mm liquid level inside (Figure 8d). The vat can be printed with any FDM printer and with typical thermoplastic such as ABS or PLA. It can also be made out of acrylics with laser cutting. Because the raised wall will block the factory building plate’s dipping motion, we further extended the building plate with a pair of rod couplers (Figure 8e). Our setup allows a printing volume of 120 mm × 68 mm × 88 mm that ensures the entire printing process is submerged in the liquid.

3.3.2 Printing with Plugs. The *Printing with Plugs* approach requires injecting hydraulic fluid after the printing but does not need hardware modification. The key is to include a threaded intake hole

and a companion plug to the hydraulic structure design (Figure 9a). The printing parameters are the same as the *Submerged Printing* technique. The printing supports are generated following the discussion of section 3.2. After printing, users can fill the printed structure (Figure 9b and c) with hydraulic fluid such as water, oil, or other liquid from the threaded hole. The companion plug can be used to block the intake.

Note that the actuation speeds of different hydraulic fluids may vary due to viscosity differences. For example, a single-generator (5-layer cylinder bellows) single-actuator (10-element bending actuator) system with either water or resin infill, can be fully actuated with 9.8 N of down-force perpendicularly applied to the generator – with the water-infilled reaches a fully actuated stage in 0.13 s vs. 2.78 s for the resin-infilled. Users may thus choose different fluids based on the need of their applications.

To ease the liquid filling process, we also suggest including a separate drain hole with the *Printing with Plugs* approach. This is to allow air to escape when filling the fluid. The drain hole can be blocked either temporarily or permanently with a drain plug to complete the system’s assembly. Since the *Printing with Plugs* method does not aim for no-assembly printing, the designer can print several components respectively and assemble them afterward. This can be useful if the hydraulic design goes beyond the volume of the printer, or the user prefer a modular design approach.



Figure 9: a) Printed parts with a drain hole and a drain plug; b) the assembled drain hole; c) the cross section of the plugged hole.

3.3.3 Comparison. The two techniques above have advantages and shortcomings against one another.

The *Submerged Printing* technique is to print ready-to-use hydraulic systems that do not need post assembly. Thus, this is convenient and time-saving, and can be suitable for applications that require fast iterations, such as design iteration and rapid prototyping. This method is most applied to advanced users due to the need for hardware modification. It also requires the user to wear gloves during operation in case of resin leakage due to over-compression; liquid resin should not directly contact the user’s skin.

The *Printing with Plugs* technique, on the other hand, does not require modification to the printer hardware and works for most SLA machines out of the box. It is arguably more friendly to users who need a modular design or essential if the hydraulic device is larger than the machine’s capacity. Users may also benefit from choosing their own hydraulic fluid. The drawback of this method is the time and labor involved for the post-printing process.

4 DESIGN SPACE, CONSIDERATION, AND GUIDELINES

In the previous section, we detailed the *FabHydro* techniques for printing key hydraulic structures. We now introduce a design space with a series of building blocks that, in all, constitute an end-to-end one-off hydraulic device (Figure 10). We categorize these building blocks following the convention of a hydraulic system, i.e., generator, transmitter, and actuator. All building blocks can be fabricated using the aforementioned printing methods.

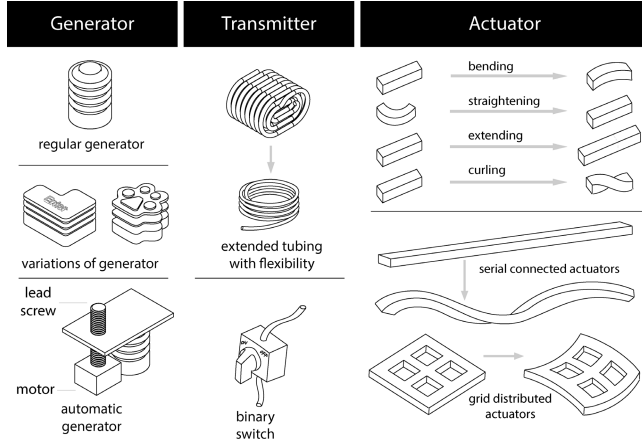


Figure 10: Design space: building blocks of *FabHydro*.

4.1 Generator

As shown in Figure 11a and b, a generator is based on the bellows structure, which in its simplest form, consists of a set of connected bags with elastic edges. Depending on the applications, generators can have different cross-section shapes (Figure 11c); can be assembled in parallel; and can be driven automatically with external forces such as an electric motor.

4.1.1 Generator Design Guideline. Here we use a primary cylindrical generator to illustrate how a designer can create proper bellows with sufficient liquid output. Figure 11d denotes the key parameters of the parametric model, including pitch (P), outer radius (OR), inner radius (IR), height (H), wall thickness (WT), and slope angle (α). The designer will first decide IR and OR of the bellows as well as H . This can help the designer to understand the maximum output volume (V) with the following equation 1.

$$V = \pi \cdot (OR - IR - WT)^2 \cdot H \quad (1)$$

The designer can also decide on bellows pitch (P), which satisfies the equation 2. Empirically, we suggest the following range for the parameters, including wall thickness (WT) from 0.8 mm to 1.5 mm, slope angle (α) from 12° to 20° , and an empirical parameter k , from 3 to 3.8. These set of parameters balance the hinge flexibility and also allow the overall structure to be stable.

$$P = 2 \tan \alpha \cdot (OR - IR) + k \cdot WT \quad (2)$$

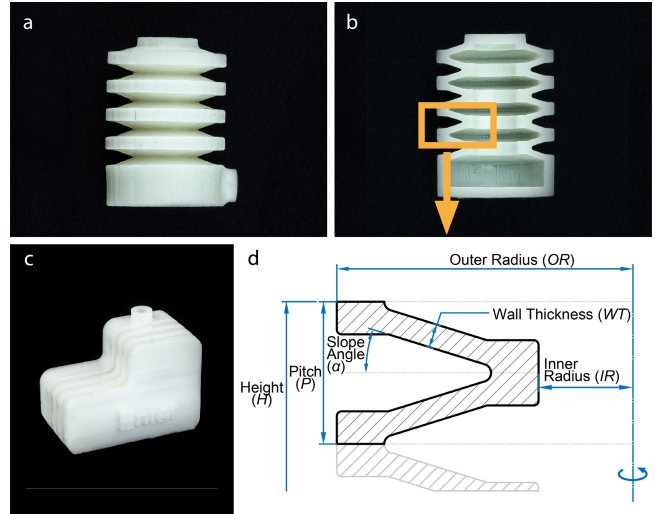


Figure 11: a) A printed generator; b) the cross-section of the printed generator; c) an example of a generator with an alternative cross-section shape; d) an illustration of the generator parameters.

4.1.2 Automated Generator. The generator can also be driven with external force, e.g., an electric motor (Figure 12). For example, here we present a design with a linear actuator set that composes two 1000 RPM gear motors with 55 mm M4 lead screws. Note that the design can scale up to accommodate different pushing volumes.

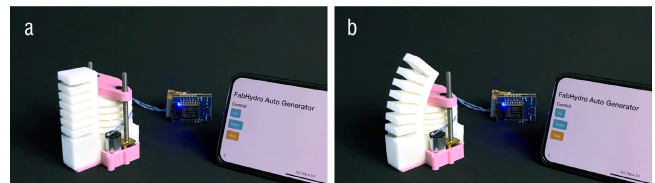


Figure 12: An example of a motor driven automatic generator: a) the automatic generator at its neutral position; the generator actuates a bending actuator.

4.2 Transmitter

A transmitter is a structural component that connects and regulates hydraulic fluids between a generator and its actuators. In our design space, transmitters are sub-categorized into tubes and switches. Tubes can come in different dimensions and lengths; switches control the on and off of the transmission. In applications requiring an actuator to stay actuated for a long time, switches will help prevent the pressure from being released.

4.2.1 Tubes. Flexible tubes (Figure 13a) can be designed and printed in various sizes. The main constraints of printing the tube coming from the printer resolution and the printer volume. Specifically, our experiment suggests that the tube’s inner diameter ID

has a lower bound of 0.5 mm when printed vertically, and 1.8 mm when printed horizontally (Figure 13b). The length of the tube is limited by the printer volume. However, by stacking helical shapes, we can print long tubes in a spiral form that can be extended after the print (Figure 13c). For a tube with the minimum ID of 3 mm, we are able to print a tube with 4.18 m length within the build volume of 68 mm × 120 mm × 70 mm (Figure 13d).

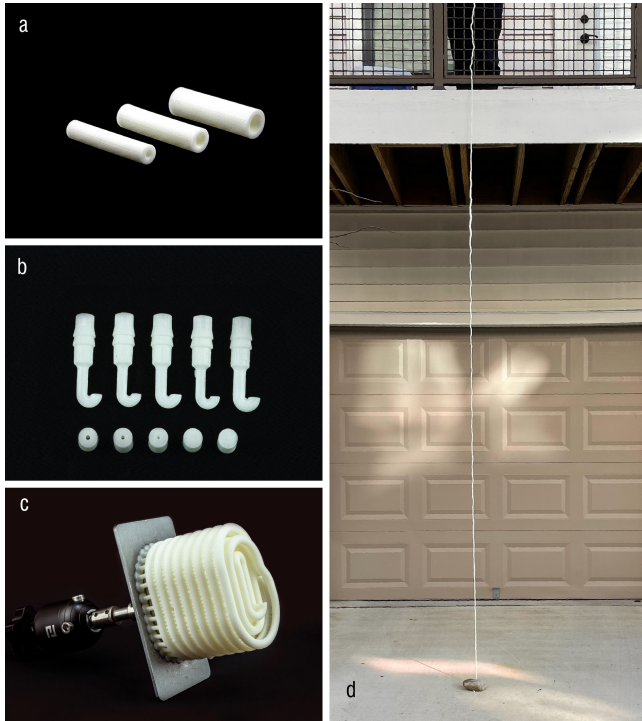


Figure 13: a) Three pieces of tube printed with different sizes; b) printed test samples that converge the minimum printable inner diameters of the tubing; c) a long tube in a spiral form; d) The long tube unfolded.

4.2.2 Switches. Using a switch can be helpful when controlling liquid flow or locking an actuator in certain poses. Here, we present a 3D printable binary switch structure that can be installed between transmitters.

Initially, we considered simple switching mechanisms such as a twist locking mechanism or a push-button to lock the liquid with static friction. However, since all components are printed with flexible materials, lockers tend to deform under pressure. Deformed

surfaces lead to reduced friction between the lockers and the transmitter holes, resulting in either liquid leaking or, in worst-case scenarios, lockers burst.

Figure 14 illustrates our final switch mechanism which is a turning knob with 3D printed threads. Threads can take a significant amount of pressure due to their increased surface area. Turning the knob towards the bottom of the locking hole on the transmitter will block the liquid flow. Disengaging the knob will resume the water flow. With the switch component, we can introduce controllability to the hydraulic systems. We can also support long-term deployment if the actuator needs to maintain a specific posture.

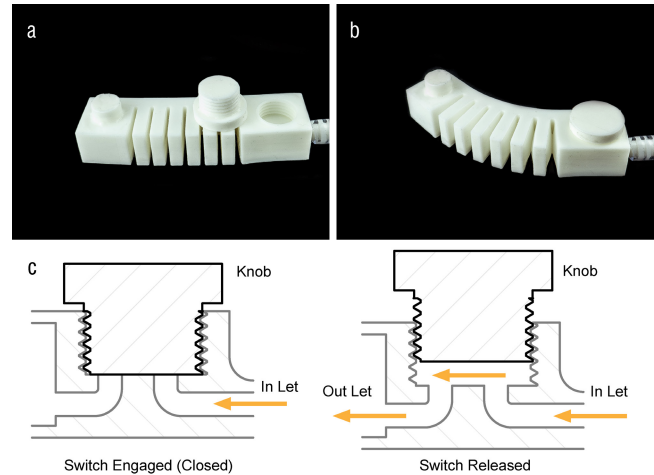


Figure 14: a) An actuator with a printed switch and a turning knob; b) an engaged switch locks the actuation in position; c) an illustration of the on-off switch in sectional view.

4.3 Actuator

Actuators are building blocks that achieve a specific posture with unevenly distributed deformation across the component. In our design space, we present the following essential deformation: bending, straightening, extending, and curling. These basic deformable building blocks can be further combined in serial or parallel for more complex actions.

4.3.1 Actuation Principle. The actuator design is inspired by the molding method in PneuNet [26] but tailored with consideration of our method’s printability and the resin property. Specifically, our actuators are designed based on small boxes with thin walls closed to each other. When pressure is applied to these boxes, the expansion of these flexible thin walls accumulates along the actuator’s

Table 2: Actuator design parameters

	Minimum Dimension (mm)	Actuation Level when Increased
<i>ThinWallThickness</i>	0.7	monotonically decrease
<i>WallSpacingDistance</i>	1.4	monotonically decrease
<i>ThinWallAreaEdgeLength</i>	6	neglectable

longitude, forming a local deformation (Figure 15). As the pressure increases, these inner walls will push the adjacent units away from each other, creating a global deformation.

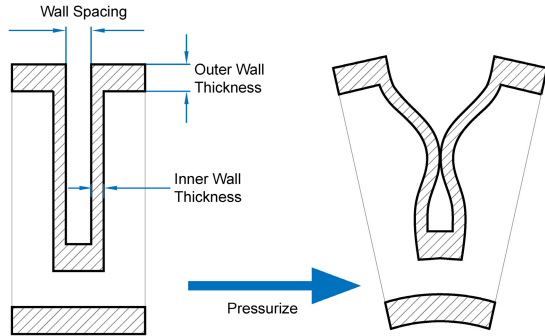


Figure 15: Expansion principle: the neutral posture with labeled design parameters (left); illustration of the pressurized expansion units (right).

4.3.2 Design Parameters. Here, we present key design parameters for working actuators, including wall thickness, distance between the expansion unit, and inner wall dimension (Figure 15).

Minimum Thin Wall Thickness. We report that the thin wall can be reliably printed with a minimum thickness of 0.7 mm. To understand the maximum pressure it can take, we further experimented with two sets of small chambers, one side printed with the 0.7 mm wall thickness and the rest with 5 mm (Figure 16a). Note that the two sets of chambers were also printed with two orientations: one with the printed layers visible across the surface (set 1) and the other with the layers parallel to the surface with no visible seam (set 2). For testing, we ran three samples for each set by pumping water into these chambers until they ruptured. The pressure was measured through a regulator. We confirm that the inner walls, even with a 0.7 mm thickness, can undertake the pressure up to 32 psi when printed in the orientation of set 1 and 33 psi for the set 2 samples.

Minimum Wall Spacing Distance. Wall spacing is the distance between each of the expansion units. We should minimize the spacing distance to achieve the maximum possible deformation. Based on our printing test, our printer’s resolution allows the minimum distance of 1.4 mm. When printing with a smaller distance, the two adjacent walls will connect occasionally.

Minimum Thin Wall Area. Another factor that affects the deformation is the expansion distance generated from the thin wall area. A longer expansion distance will push the adjacent units further away from each other, resulting in a more aggressive overall deformation. In this experiment, we altered the thin wall area to observe the changes of the expansion distance (Figure 16b). Specifically, we printed a series of chambers with one wall with 0.7 mm thick and the rest with 5 mm, the same as in the previous experiment. The

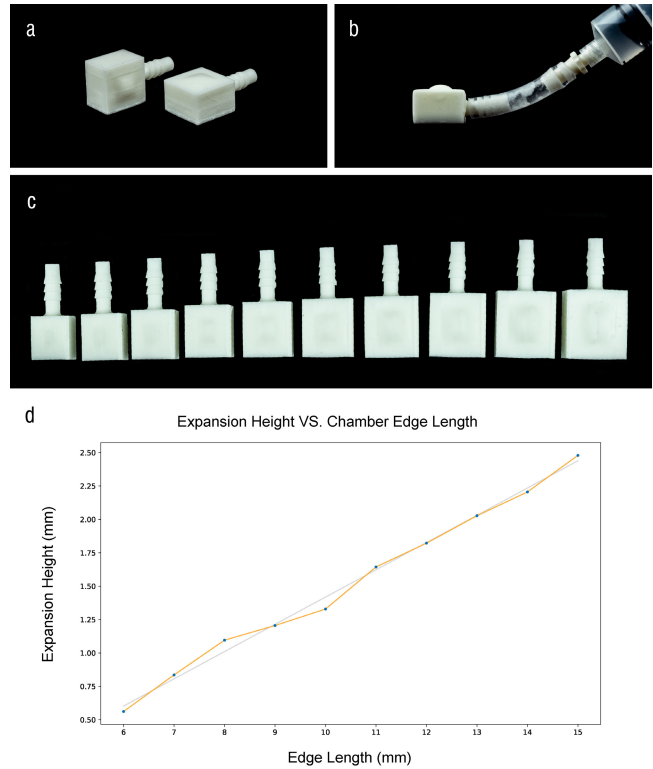


Figure 16: Expansion experiment: a) chambers printed in both orientations; b) the expansion of a 6 mm edge length unit; c) samples from 6 -15 mm edge length; d) the expansion height is approximately linear against the edge length.

cross-section area is a square shape, thus the size of the area is controlled by the edge length, which ranges from 6 mm to 15 mm, with 1 mm increments (Figure 16c). Pressurized water was pumped into the chambers with 20 psi (Figure 16b). The vertical expansion height is shown in the graph (Figure 16d). According to the result, we conclude that the maximum expansion height is approximately linear against the edge length of the inner wall. When considering together with the wall spacing (see above), we can conclude that the thin wall should have edges not smaller than 6 mm.

The above design parameters are summarized in Table 2.

4.3.3 Actuator design. By altering the expansion units placement, a designer can achieve a wide range of deformation behaviors. For example, when multiple expansion units are placed along a straight line, we can create a bending actuator (Figure 17a); when the expansion units are allocated along a curve, bending angles can be straightened (Figure 17b); when the expansion units are distributed in a zig-zag pattern, a pair of expansion units will counter-balance each other, creating a global expansion (Figure 17c); when an array of the expansion units connected at an angle, we make a curling actuator (Figure 17d). To achieve a more complex actuation, multiple actuators can be connected in serial or parallel. Figure 18 shows two such examples.

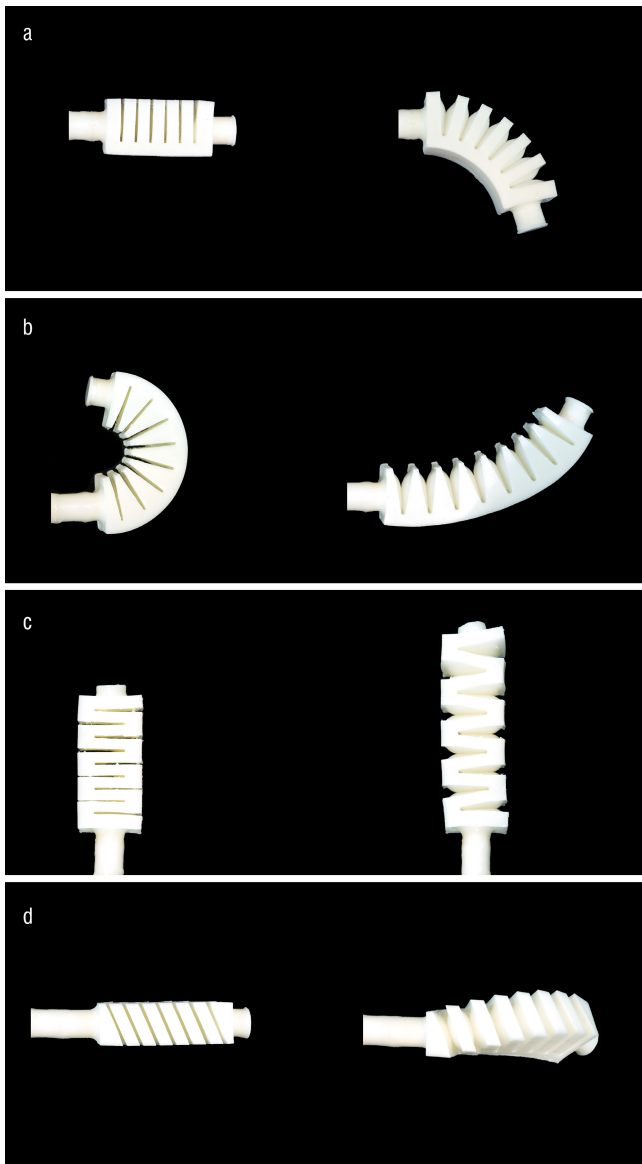


Figure 17: Basic Actuators: a) bending actuator; b) straightening actuator; c) extending actuator; d) curling actuator.

5 APPLICATIONS

To illustrate the potential of our approach and highlight our design space, we showcase five applications, each emphasizing one or more features of *FabHydro*.

5.1 Folding Lamp

In this example, we show a portable folding lamp with adjustable postures (Figure 19). The lamp is printed one-off, with one cylinder generator, one straightening actuator, and locked-in transmission fluid, using the *Submerged Printing* technique (Figure 19a). When the user presses the generator, the lamp will unfold and light up

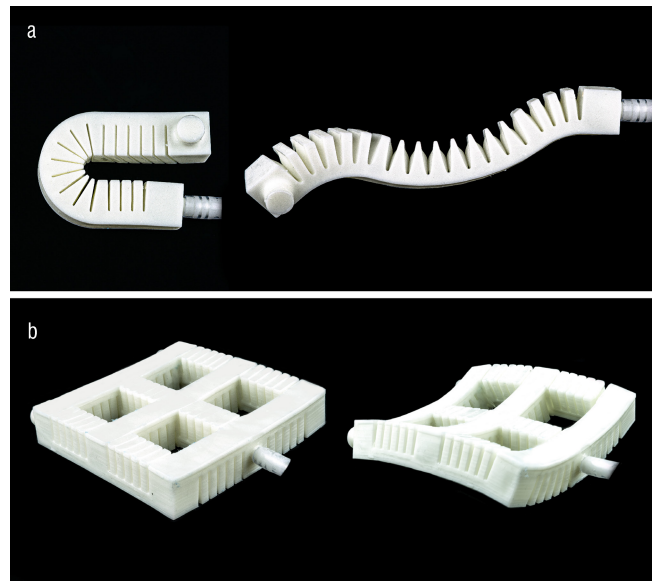


Figure 18: a) A serially connected actuator with a bending, straightening and curling actuator, respectively; b) four bending actuators distributed in a two by two grid form a saddle shape when actuated.

(Figure 19b). The user can adjust the amount of unfolding by pressing the generator to different heights. An LED is attached to the lamp with copper tapes, which close the circuit when actuation happens.

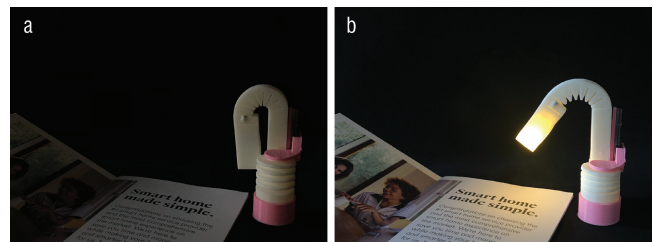


Figure 19: A printed folding Lamp a) is off at its neutral posture and b) lights up with actuation.

5.2 Robotic Gripper with Distant Control

One of the benefits of a hydraulic device is that the force applied at a remote place can be transmitted with minimal loss. To demonstrate this benefit, we designed a robotic gripper with haptic control that can potentially allow handling hazardous materials from a distance. As shown in Figure 20a, a two-finger robotic gripper is attached to a collaborative robotic arm. Each of the fingers is embedded with a bending actuator. Two printed tubes are extended from the gripper's mounting plate. On the other end of the tubes are cylinder generators that drive the gripper fingers. As we can see from Figure

20b and c, the grippers still maintain the strength of carrying a cake even with the 3.3 m long transmission distance.



Figure 20: The printed robotic gripper: a) the printed assembly is installed to an UR3 robotic arm; b) the gripper aims for the cake; c) the gripper is activated to lift the cake with the operator at a distance.

5.3 Augmented Fluffy Elephant

In this example, we augment a fluffy toy with controllable motions. We include a printed switch that was introduced in the design space to enable binary controls of the elephant's actions (Figure 21a). The switch helps connect and disconnect channels in the system with a twisting knob. In this example, two straightening actuators are used to activate the arms of the elephant, and one bending actuator is printed to control the trunk. The user can choose to actuate all three actuators at once or actuate them individually by turning the switch on or off (Figure 21b, c and d).

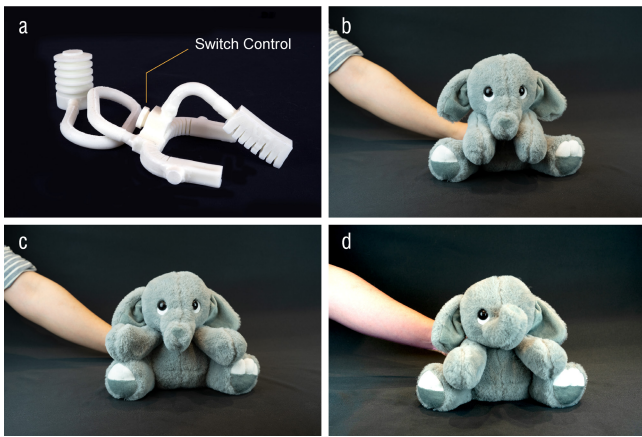


Figure 21: A fluffy elephant can be activated with the printed hydraulic device: a) the printed device to be embedded in the elephant toy; b) the neutral posture of the elephant; c) the elephant with its arms actuated; d) both the elephant's arms and its trunk are actuated.

5.4 Phone Stand as an Ambient and Tangible Display

Inspired by recent work on tangible actuators ([22, 27]), we showcase an active phone stand that sends notifications to the user with its tangible motions. The phone stand will rise when the user has an incoming call. It will then alter its bending angle, creating a



Figure 22: a) The phone stand hydraulic system; b) the neutral posture of the phone stand assembly with an automatic generator; c) the ambient interface indicating an incoming call.

'breathing' effect as an ambient display [21] (Figure 22c). Unlike previous examples, the phone stand's actuator is designed with widened cross-section to hold the phone properly (Figure 22a). The expansion units are also not evenly distributed. Instead, the distance increases gradually, creating a bending surface with tangent continuity at the top. Actuation is achieved with a motor-driven generator (Figure 22b).

5.5 Tangibles for Collaborative Game

In this example, we demonstrate a collaborative game with printed tangibles. Two gamers each will control a push-button generator (Figure 23b) — a generator with a custom shape of a cat paw (Figure 23a). The height changes of the two buttons will jointly decide a tangible prop's location on a touch screen (Figure 23c), of which a fishing game is displayed. The game's goal is for the two users to catch fish by placing the fishing prop at the correct location (Figure 23d). In this example, the tangible prop is designed with a shared connection to two parallel extending actuators; each actuator is then connected to the cat paw generator. The game interface is programmed with Processing.

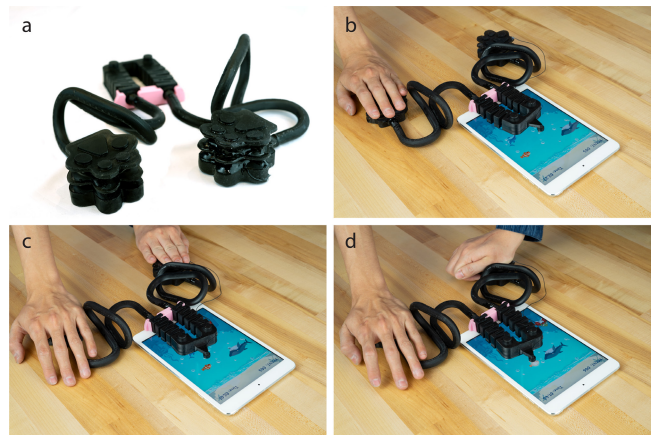


Figure 23: a) The game control with two cat paw generators in parallel; b) When activating one generator, the prop bends towards one direction; c) two users need to collaboratively control their generators so that the tangible prop can hit the fish; d) users successfully catch a fish and gain a point.

6 DISCUSSION

FabHydro enables a rapid, low-cost approach to fabricate hydraulic devices using a desktop SLA 3D printer. We now discuss some aspects of our approach that warrant further research efforts.

6.1 Pneumatic VS. Hydraulic

In this work, we adopted hydraulic transmission over pneumatic for two reasons.

First, a hydraulic mechanism is more energy efficient. We compared both methods' transmission efficiency by printing two sets of single-actuator-single-generator systems with an identical design. We filled one system with water and sealed the other with air. Upon full compression of the generator, the hydraulic-driven system's actuation has a more significant displacement (figure 24). This is caused by the non-linearity of the volume-pressure relationship in the pneumatic systems. Similar effects can be seen in balloons where the air volume increases, but the pressure tends to remain stable.

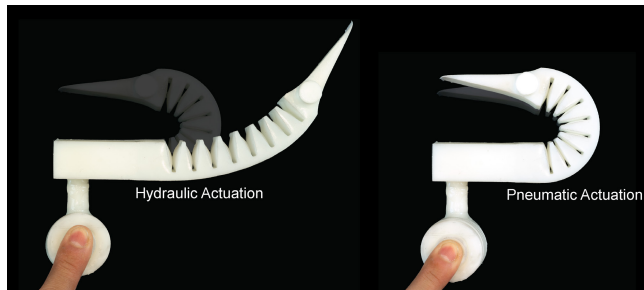


Figure 24: Pneumatic vs. hydraulic: the actuation achieved with hydraulic fluid (left); the actuation achieved with the pneumatic setup has a smaller displacement (right).

Second, pneumatic and hydraulic systems use different sources of actuation. To achieve similar actuation, a pneumatic system needs a much bigger generator than that of a hydraulic system, or a pre-pressurized inner chamber with an external air inlet and a pump. As a result, a pneumatic system can be bulky and much louder than a hydraulic based system. The latter thus may be more suitable for small-size actuation mechanisms that are often used in the HCI field.

6.2 How Long Will It Last

The UV-sensitive resin will cure when exposed to UV light. One of the main concerns we have for a printed hydraulic device, especially with the *Submerged Printing* approach, is that the liquid resin may get cured after the object is printed.

To understand how long the printed object will still be functional under normal indoor usage, we ran an exposure experiment for a series of printed cubes that all have locked-in resin. Specifically, we printed 48 testing cubes with the side length of 11 mm and wall thickness of 1 mm using the *Submerged Printing* process. All samples were placed in an indoor environment with a light intensity of 400 to 600 lux. Every 24 hours, we cut open three cubes to measure how much of the resin was still in the liquid phase by weighting the

cube before and after the cut, as shown in Figure 25a. Figure 25b shows the result of the 16-day experiment. Over time, we observe that the liquid resin does get cured gradually, but mainly close to the wall. The amount of cured resin reaches stability at day eight, with still more than 75% of resin remains in the liquid phase. Thus, our printing method is proper for rapid prototyping. Increasing the wall thickness can further reduce the fluid loss, but at the cost of losing flexibility.

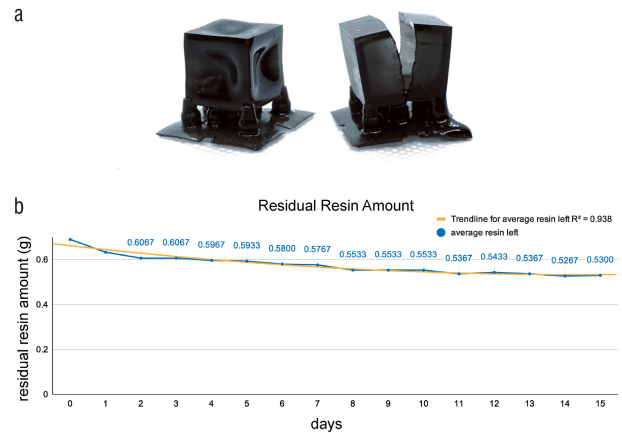


Figure 25: The exposure experiment result: a) experiment samples; b) residual liquid resin reaches stability at day eight.

6.3 Printing Time and Size

For an LCD-SLA printer, the typical exposure time for one layer is 7 to 9s. In our method, we raise the layer exposure time to the 30s. We also reduce the lifting speed from 90 to 55 mm/min, making the entire printing process four times longer than the default setting. For example, the 40 mm tall example in Figure 2a takes up to 4.5 hours to finish. The printing time can be reduced partially with a stronger UV light source. For example, recent LCD-SLA 3D printers such as the Elegoo Mars 2 Pro [7] uses a monochrome light source, which can shorten the entire printing time to half. The size of the printing plate is another limitation. With our current hardware, many designs cannot be printed at once and thus require assembly. For example, the robotic gripper design (Figure 20) has two long tubes, but the printing plate can only accommodate one tube at a time. Thus the size of the plate requires us to print two batches separately. An increasing number of large-scale SLA 3D printers are now available with a printing plate up to 270 mm × 290 mm × 475 mm, more than eight times bigger than our current hardware. This will reduce the amount of the required assembly and open up new design opportunities.

6.4 Designer Tool Kit

The main goal of this work is to explore the fabrication process for low-cost interactive hydraulic devices. As such, we reported key fabrication techniques as well as the design space and guidance to

ensure printable hydraulic components. Moving forward, we aim to embrace the full potential of *FabHydro* by offering a designer toolkit. As a starting point, we have developed a Rhino 6 slicer plugin to generate the panel support with previewed deformation (Figure 26). This is achieved by converting and simplifying the input geometry to triangle meshes and then applying FEA [34] to the converted structure. In the future, we will include parametric design features that allow designers to quickly connect different hydraulic components and add real-time simulations of the actuation result.

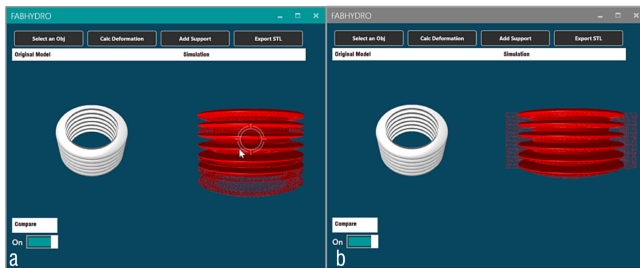


Figure 26: A work-in-progress slicer plugin: a) the software calculates the displacement and visualized in Red triangular meshes; b) the software generates the support panel and performs FEA.

7 CONCLUSION

In this paper, we present *FabHydro*, a rapid and low-cost method to print hydraulic devices with an off-the-shelf SLA 3D printer. Sealed 3D structures can be printed either submerged or with plugs using flexible photosensitive resin and custom panel supports. We report a design space with a series of building blocks for the hydraulic generator, transmitter, and actuator. We show the breadth of our approach with a list of examples. With the low-cost setup and accessible workflow, we hope our work can further enrich the design for 3D printed interactive devices.

ACKNOWLEDGMENTS

We thank Anup Sathya Sai Kumar and Jiasheng Li for their time and efforts with video shooting. We also thank reviewers for their valuable feedback.

REFERENCES

- [1] Byoungkwon An, Ye Tao, Jianzhe Gu, Tingyu Cheng, Xiang 'Anthony' Chen, Xiaoxiao Zhang, Wei Zhao, Youngwook Do, Shigeo Takahashi, Hsiang-Yun Wu, Teng Zhang, and Lining Yao. 2018. Thermorph: Democratizing 4D Printing of Self-Folding Materials and Interfaces. In *Proceedings of the 2018 CHI Conference on Human Factors in Computing Systems*. Association for Computing Machinery, New York, NY, USA, 1–12. <https://doi.org/10.1145/3173574.3173834>
- [2] Daniel Ashbrook, Shitao Stan Guo, and Alan Lambie. 2016. Towards Augmented Fabrication: Combining Fabricated and Existing Objects. In *Proceedings of the 2016 CHI Conference Extended Abstracts on Human Factors in Computing Systems* (San Jose, California, USA) (CHI EA '16). Association for Computing Machinery, New York, NY, USA, 1510–1518. <https://doi.org/10.1145/2851581.2892509>
- [3] Eric Brockmeyer, Ivan Poupyrev, and Scott Hudson. 2013. PAPILLON: Designing Curved Display Surfaces with Printed Optics. In *Proceedings of the 26th Annual ACM Symposium on User Interface Software and Technology* (St. Andrews, Scotland, United Kingdom) (UIST '13). Association for Computing Machinery, New York, NY, USA, 457–462. <https://doi.org/10.1145/2501988.2502027>
- [4] Jesse Burstyn, Nicholas Fellion, Paul Strohmeier, and Roel Vertegaal. 2015. Print-Put: Resistive and Capacitive Input Widgets for Interactive 3D Prints. In *Human-Computer Interaction – INTERACT 2015*, Julio Abascal, Simone Barbosa, Mirko Fetter, Tom Gross, Philippe Palanque, and Marco Winckler (Eds.). Springer International Publishing, Cham, 332–339. https://doi.org/10.1007/978-3-319-22701-6_25
- [5] Youngkyung Choi, Neung Ryu, Myung Jin Kim, Artem Dementyev, and Andrea Bianchi. 2020. BodyPrinter: Fabricating Circuits Directly on the Skin at Arbitrary Locations Using a Wearable Compact Plotter. In *Proceedings of the 33rd Annual ACM Symposium on User Interface Software and Technology*. Association for Computing Machinery, New York, NY, USA, 554–564. <https://doi.org/10.1145/3379337.3415840>
- [6] Kahraman G. Demir, Zhizhou Zhang, Jehan Yang, and Grace X. Gu. 2020. Computational and Experimental Design Exploration of 3D-Printed Soft Pneumatic Actuators. *Advanced Intelligent Systems* 2, 7 (2020), 2000013. <https://doi.org/10.1002/aisy.202000013>
- [7] Elegoo. 2020. Elegoo Mars 2 Pro 3D Printer. <https://www.elegoo.com/products/elegoo-mars-2-pro-mono-lcd-3d-printer>.
- [8] Elegoo. 2020. Elegoo Mars LCD-SLA 3D Printer. <https://www.elegoo.com/products/elegoo-mars-lcd-3d-printer>.
- [9] Elegoo. 2020. Photopolymer Resin Material Data Sheet. <https://www.elegoo.com/blogs/3d-printing/elegoo-resin-sds>.
- [10] Anthony Esposito. 2000. *Fluid power with applications*. Prentice-Hall International Upper Saddle River.
- [11] Jack Forman, Mustafa Doga Dogan, Hamilton Forsythe, and Hiroshi Ishii. 2020. DefeXtiles: 3D Printing Quasi-Woven Fabric via Under-Extrusion. In *Proceedings of the 33rd Annual ACM Symposium on User Interface Software and Technology*. Association for Computing Machinery, New York, NY, USA, 1222–1233. <https://doi.org/10.1145/3379337.3415876>
- [12] Wei Gao, Yunbo Zhang, Diogo C. Nazzetta, Karthik Ramani, and Raymond J. Cipra. 2015. RevoMaker: Enabling Multi-Directional and Functionally-Embedded 3D Printing Using a Rotational Cuboidal Platform. In *Proceedings of the 28th Annual ACM Symposium on User Interface Software and Technology* (Charlotte, NC, USA) (UIST '15). Association for Computing Machinery, New York, NY, USA, 437–446. <https://doi.org/10.1145/2807442.2807476>
- [13] Jianzhe Gu, David E. Breen, Jenny Hu, Lifeng Zhu, Ye Tao, Tyson Van de Zande, Guanyun Wang, Yongjie Jessica Zhang, and Lining Yao. 2019. Geodesy: Self-Rising 2.5D Tiles by Printing along 2D Geodesic Closed Path. In *Proceedings of the 2019 CHI Conference on Human Factors in Computing Systems*. Association for Computing Machinery, New York, NY, USA, 1–10. <https://doi.org/10.1145/3290605.3300267>
- [14] Liang He, Huaishu Peng, Michelle Lin, Ravikanth Konjeti, François Guimbretière, and Jon E. Froehlich. 2019. Ondulé: Designing and Controlling 3D Printable Springs. In *Proceedings of the 32nd Annual ACM Symposium on User Interface Software and Technology* (New Orleans, LA, USA) (UIST '19). Association for Computing Machinery, New York, NY, USA, 739–750. <https://doi.org/10.1145/3332165.3347951>
- [15] Jonathan Hook, Thomas Nappey, Steve Hodges, Peter Wright, and Patrick Olivier. 2014. Making 3D Printed Objects Interactive Using Wireless Accelerometers. In *CHI '14 Extended Abstracts on Human Factors in Computing Systems*. Association for Computing Machinery, New York, NY, USA, 1435–1440. <https://doi.org/10.1145/2559206.2581137>
- [16] Alexandra Ion, Johannes Frohnhofen, Ludwig Wall, Robert Kovacs, Mirela Alistar, Jack Lindsay, Pedro Lopes, Hsiang-Ting Chen, and Patrick Baudisch. 2016. Metamaterial Mechanisms. In *Proceedings of the 29th Annual Symposium on User Interface Software and Technology* (Tokyo, Japan) (UIST '16). Association for Computing Machinery, New York, NY, USA, 529–539. <https://doi.org/10.1145/2984511.2984540>
- [17] Alexandra Ion, Robert Kovacs, Oliver S. Schneider, Pedro Lopes, and Patrick Baudisch. 2018. Metamaterial Textures. In *Proceedings of the 2018 CHI Conference on Human Factors in Computing Systems*. Association for Computing Machinery, New York, NY, USA, 1–12. <https://doi.org/10.1145/3173574.3173910>
- [18] Alexandra Ion, David Lindlbauer, Philipp Herholz, Marc Alexa, and Patrick Baudisch. 2019. Understanding Metamaterial Mechanisms. In *Proceedings of the 2019 CHI Conference on Human Factors in Computing Systems*. Association for Computing Machinery, New York, NY, USA, 1–14. <https://doi.org/10.1145/3290605.3300877>
- [19] Alexandra Ion, Ludwig Wall, Robert Kovacs, and Patrick Baudisch. 2017. Digital Mechanical Metamaterials. In *Proceedings of the 2017 CHI Conference on Human Factors in Computing Systems*. Association for Computing Machinery, New York, NY, USA, 977–988. <https://doi.org/10.1145/3025453.3025624>
- [20] Yoshio Ishiguro and Ivan Poupyrev. 2014. 3D Printed Interactive Speakers. In *Proceedings of the SIGCHI Conference on Human Factors in Computing Systems* (Toronto, Ontario, Canada) (CHI '14). Association for Computing Machinery, New York, NY, USA, 1733–1742. <https://doi.org/10.1145/2556288.2557046>
- [21] Hiroshi Ishii and Brygg Ullmer. 1997. Tangible Bits: Towards Seamless Interfaces between People, Bits and Atoms. In *Proceedings of the ACM SIGCHI Conference on Human Factors in Computing Systems* (Atlanta, Georgia, USA) (CHI '97). Association for Computing Machinery, New York, NY, USA, 234–241. <https://doi.org/10.1145/258549.258715>

- [22] Miyu Iwafune, Taisuke Ohshima, and Yoichi Ochiai. 2016. Coded Skeleton: Programmable Deformation Behaviour for Shape Changing Interfaces. In *SIGGRAPH ASIA 2016 Emerging Technologies* (Macau) (SA '16). Association for Computing Machinery, New York, NY, USA, Article 1, 2 pages. <https://doi.org/10.1145/2988240.2988252>
- [23] Shohei Katakura, Yuto Kuroki, and Keita Watanabe. 2019. A 3D Printer Head as a Robotic Manipulator. In *Proceedings of the 32nd Annual ACM Symposium on User Interface Software and Technology* (New Orleans, LA, USA) (UIST '19). Association for Computing Machinery, New York, NY, USA, 535–548. <https://doi.org/10.1145/3332165.3347885>
- [24] Gierad Laput, Xiang 'Anthony' Chen, and Chris Harrison. 2015. 3D Printed Hair: Fused Deposition Modeling of Soft Strands, Fibers, and Bristles. In *Proceedings of the 28th Annual ACM Symposium on User Interface Software and Technology* (Charlotte, NC, USA) (UIST '15). Association for Computing Machinery, New York, NY, USA, 593–597. <https://doi.org/10.1145/2807442.2807484>
- [25] Robert MacCurdy, Robert Katzschmann, Youbin Kim, and Daniela Rus. 2016. Printable hydraulics: A method for fabricating robots by 3D co-printing solids and liquids. In *2016 IEEE International Conference on Robotics and Automation (ICRA)*. 3878–3885. <https://doi.org/10.1109/ICRA.2016.7487576>
- [26] Bobak Mosadegh, Panagiotis Polygerinos, Christoph Keplinger, Sophia Wennstedt, Robert F. Shepherd, Unmukt Gupta, Jongmin Shim, Katia Bertoldi, Conor J. Walsh, and George M. Whitesides. 2014. Pneumatic Networks for Soft Robotics that Actuate Rapidly. *Advanced Functional Materials* 24, 15 (2014), 2163–2170. <https://doi.org/10.1002/adfm.201303288>
- [27] Ryosuke Nakayama, Ryo Suzuki, Satoshi Nakamaru, Ryuma Niiyama, Yoshihiro Kawahara, and Yasuaki Kakehi. 2019. MorphIO: Entirely Soft Sensing and Actuation Modules for Programming Shape Changes through Tangible Interaction. In *Proceedings of the 2019 on Designing Interactive Systems Conference* (San Diego, CA, USA) (DIS '19). Association for Computing Machinery, New York, NY, USA, 975–986. <https://doi.org/10.1145/3322276.3322337>
- [28] Yuta Noma, Koya Narumi, Fuminori Okuya, and Yoshihiro Kawahara. 2020. Pop-up Print: Rapidly 3D Printing Mechanically Reversible Objects in the Folded State. In *Proceedings of the 33rd Annual ACM Symposium on User Interface Software and Technology*. Association for Computing Machinery, New York, NY, USA, 58–70. <https://doi.org/10.1145/3379337.3415853>
- [29] Jifei Ou, Gershon Dublon, Chin-Yi Cheng, Felix Heibeck, Karl Willis, and Hiroshi Ishii. 2016. Cillia: 3D Printed Micro-Pillar Structures for Surface Texture, Actuation and Sensing. In *Proceedings of the 2016 CHI Conference on Human Factors in Computing Systems*. Association for Computing Machinery, New York, NY, USA, 5753–5764. <https://doi.org/10.1145/2858036.2858257>
- [30] Andrew Parr. 2011. *Hydraulics and pneumatics: a technician's and engineer's guide*. Elsevier. <https://doi.org/10.1016/C2009-0-64113-1>
- [31] Bryan N Peele, Thomas J Wallin, Huichan Zhao, and Robert F Shepherd. 2015. 3D printing antagonistic systems of artificial muscle using projection stereolithography. *Bioinspiration & Biomimetics* 10, 5 (sep 2015), 055003. <https://doi.org/10.1088/1748-3190/10/5/055003>
- [32] Huaishu Peng, François Guimbretière, James McCann, and Scott Hudson. 2016. A 3D Printer for Interactive Electromagnetic Devices. In *Proceedings of the 29th Annual Symposium on User Interface Software and Technology* (Tokyo, Japan) (UIST '16). Association for Computing Machinery, New York, NY, USA, 553–562. <https://doi.org/10.1145/2984511.2984523>
- [33] Huaishu Peng, Jennifer Mankoff, Scott E. Hudson, and James McCann. 2015. A Layered Fabric 3D Printer for Soft Interactive Objects. In *Proceedings of the 33rd Annual ACM Conference on Human Factors in Computing Systems*. Association for Computing Machinery, New York, NY, USA, 1789–1798. <https://doi.org/10.1145/2702123.2702327>
- [34] Clemens Preisinger and Moritz Heimrath. 2014. Karamba—A Toolkit for Parametric Structural Design. *Structural Engineering International* 24, 2 (2014), 217–221. <https://doi.org/10.2749/101686614X13830790993483>
- [35] RESIONE. 2020. RESIONE F39/F69 Material Datasheet. http://en.godsaid3d.com/?attachment_id=17671.
- [36] Michael L. Rivera and Scott E. Hudson. 2019. Desktop Electrospinning: A Single Extruder 3D Printer for Producing Rigid Plastic and Electrospun Textiles. In *Proceedings of the 2019 CHI Conference on Human Factors in Computing Systems*. Association for Computing Machinery, New York, NY, USA, 1–12. <https://doi.org/10.1145/3290605.3300434>
- [37] Valkyrie Savage, Colin Chang, and Björn Hartmann. 2013. Sauron: Embedded Single-Camera Sensing of Printed Physical User Interfaces. In *Proceedings of the 26th Annual ACM Symposium on User Interface Software and Technology* (St. Andrews, Scotland, United Kingdom) (UIST '13). Association for Computing Machinery, New York, NY, USA, 447–456. <https://doi.org/10.1145/2501988.2501992>
- [38] Valkyrie Savage, Sean Follmer, Jingyi Li, and Björn Hartmann. 2015. Makers' Marks: Physical Markup for Designing and Fabricating Functional Objects. In *Proceedings of the 28th Annual ACM Symposium on User Interface Software and Technology* (Charlotte, NC, USA) (UIST '15). Association for Computing Machinery, New York, NY, USA, 103–108. <https://doi.org/10.1145/2807442.2807508>
- [39] Martin Schmitz, Mohammadreza Khalilbeigi, Matthias Balwierz, Roman Lissermann, Max Mühlhäuser, and Jürgen Steimle. 2015. Capricate: A Fabrication Pipeline to Design and 3D Print Capacitive Touch Sensors for Interactive Objects. In *Proceedings of the 28th Annual ACM Symposium on User Interface Software and Technology* (Charlotte, NC, USA) (UIST '15). Association for Computing Machinery, New York, NY, USA, 253–258. <https://doi.org/10.1145/2807442.2807503>
- [40] Jun Shintake, Vito Cacucciolo, Dario Floreano, and Herbert Shea. 2018. Soft Robotic Grippers. *Advanced Materials* 30, 29 (2018), 1707035. <https://doi.org/10.1002/adma.201707035>
- [41] Mark A. Skylar-Scott, Jochen Mueller, Claas W. Visser, and Jennifer A. Lewis. 2019. Voxlated soft matter via multimaterial multinozzle 3D printing. *Nature* 575, 7782 (01 Nov 2019), 330–335. <https://doi.org/10.1038/s41586-019-1736-8>
- [42] Stratasys. 2020. Stratasys Objet30 3D printer. https://www.stratasys.com/-/media/files/printer-spec-sheets/ps_pj_objet30v5_1020a.pdf.
- [43] Pavol Suly, Jakub Sevcik, David J. Dmonte, Pavel Urbanek, and Ivo Kuritka. 2021. Inkjet Printability Assessment of Weakly Viscoelastic Fluid: A Semidilute Polyvinylpyrrolidone Solution Ink Case Study. *Langmuir* 37, 28 (2021), 8557–8568. <https://doi.org/10.1021/acs.langmuir.1c01010> PMID: 34233120
- [44] Haruki Takahashi and Jeeun Kim. 2019. 3D Printed Fabric: Techniques for Design and 3D Weaving Programmable Textiles. In *Proceedings of the 32nd Annual ACM Symposium on User Interface Software and Technology* (New Orleans, LA, USA) (UIST '19). Association for Computing Machinery, New York, NY, USA, 43–51. <https://doi.org/10.1145/3332165.3347896>
- [45] Siraya Tech. 2020. Tenacious Impact Resistant Resin. <https://siraya.tech/products/tenacious-by-siraya-tech-for-lcd-resin-3d-printers-1kg>.
- [46] Tatyana Vasilevitsky and Amit Zoran. 2016. Steel-Sense: Integrating Machine Elements with Sensors by Additive Manufacturing. In *Proceedings of the 2016 CHI Conference on Human Factors in Computing Systems*. Association for Computing Machinery, New York, NY, USA, 5731–5742. <https://doi.org/10.1145/2858036.2858309>
- [47] T. J. Wallin, J. Pikul, and R. F. Shepherd. 2018. 3D printing of soft robotic systems. *Nature Reviews Materials* 3, 6 (01 Jun 2018), 84–100. <https://doi.org/10.1038/s41578-018-0002-2>
- [48] Guanyun Wang, Ye Tao, Ozguc Bertug Capunaman, Humphrey Yang, and Lining Yao. 2019. A-Line: 4D Printing Morphing Linear Composite Structures. In *Proceedings of the 2019 CHI Conference on Human Factors in Computing Systems*. Association for Computing Machinery, New York, NY, USA, 1–12. <https://doi.org/10.1145/3290605.3300656>
- [49] Guanyun Wang, Humphrey Yang, Zeyu Yan, Nurcan Gecer Ulu, Ye Tao, Jianzhe Gu, Levent Burak Kara, and Lining Yao. 2018. 4DMesh: 4D Printing Morphing Non-Developable Mesh Surfaces. In *Proceedings of the 31st Annual ACM Symposium on User Interface Software and Technology* (Berlin, Germany) (UIST '18). Association for Computing Machinery, New York, NY, USA, 623–635. <https://doi.org/10.1145/3242587.3242625>
- [50] Guanyun Wang, Lining Yao, Wen Wang, Jifei Ou, Chin-Yi Cheng, and Hiroshi Ishii. 2016. XPrint: A Modularized Liquid Printer for Smart Materials Deposition. In *Proceedings of the 2016 CHI Conference on Human Factors in Computing Systems*. Association for Computing Machinery, New York, NY, USA, 5743–5752. <https://doi.org/10.1145/2858036.2858281>
- [51] Karl Willis, Eric Brockmeyer, Scott Hudson, and Ivan Poupyrev. 2012. Printed Optics: 3D Printing of Embedded Optical Elements for Interactive Devices. In *Proceedings of the 25th Annual ACM Symposium on User Interface Software and Technology* (Cambridge, Massachusetts, USA) (UIST '12). Association for Computing Machinery, New York, NY, USA, 589–598. <https://doi.org/10.1145/2380116.2380190>
- [52] Junyi Zhu, Lotta-Gili Blumberg, Yunyi Zhu, Martin Nisser, Ethan Levi Carlson, Xin Wen, Kevin Shum, Jessica Ayeley Quayay, and Stefanie Mueller. 2020. CurveBoards: Integrating Breadboards into Physical Objects to Prototype Function in the Context of Form. In *Proceedings of the 2020 CHI Conference on Human Factors in Computing Systems*. Association for Computing Machinery, New York, NY, USA, 1–13. <https://doi.org/10.1145/3313831.3376617>